

2006 Best Paper 1 - Numerical and Experimental Study of Dispersive Mixing of Agglomerates

[Print](#)

[\(10\)](#) » [2008 Best Paper - Multilayer Rheology Effects in Coextruded Structure Design](#) » [2007 Best Paper - Determining the Processability of Multilayer Coextruded Structures](#) » [2006 Best Paper 1 - Numerical and Experimental Study of Dispersive Mixing of Agglomerates](#)

Numerical and Experimental Study of Dispersive Mixing of Agglomerates

V. Collin^{1*}, E. Peuvrel-Disdier¹, B. Alsteens^{2**}, V. Legat², T. Avalosse³, S. Otto⁴, and H. M. Metwally⁵

¹ - Ecole des Mines de Paris, Centre de Mise en Forme des Matériaux, UMR CNRS / Ecole des Mines de Paris N°7635, BP207, F-06904 Sophia-Antipolis, France.

² - University of Louvain, Center for Systems Engineering and Applied Mechanics (CESAME) Av. Georges Lemaître 4, B-1348 Louvain-la-Neuve, Belgium.

³ - Fluent Benelux, Av. Pasteur 4, B-1300 Wavre, Belgium.

⁴ - Manufacture Française des Pneumatiques Michelin, Place des Carmes Dechaux, F-63040 Clermont-Ferrand, France.

⁵ - Fluent USA Inc, 1007 Church Street, Ste. 250, Evanston, IL 60201.

. * Present address: Lafarge Centre de Recherche, rue du Montmurier 95, BP 15, 38291 St Quentin Fallavier Cedex, France

. ** Present address: LMS, Researchpark Z1, Interleuvenlaan 68, B-3001 Leuven, Belgium

Abstract

The degree of filler dispersion has a major influence on the physical properties of rubber compounds. Typical fillers, e.g. carbon black and silica, are difficult to disperse, particularly if they are fine and low structured. As a result, the quantity of undispersed fillers generally amounts for 1% to 10% of the compound. The elimination, or at least the reduction, of agglomerates will result in rubber parts (e.g. tires, seals, belts) with improved properties and higher reliability. Clearly, a better understanding of the physics of batch mixers would help improve their mixing performance. Due to the complexity of the real process, experiments on a representative device were held from which a model has been deduced. It appears to be a generalization of the law of Kao and Mason, but for high viscous matrices. The next step was to get a model available for statistically large number of pellets as can be found in any sample taken out of the mixer. A statistical approach is used where we define a model describing the evolution of mass density function of agglomerate sizes. Eventually, we implement this model within available numerical simulation tools to estimate dispersion in real mixers.

INTRODUCTION

Fillers like carbon black or silica are mixed with rubber to improve various mechanical properties. However, the final state of the mixture directly affects the quality and life duration of the final product [1]. Despite continuous improvements, the actual mixers do not disperse all pellets down to sub-micron aggregates. To increase the performances of mixers, a better understanding of the dispersion mechanisms is necessary. In the following study, a model of dispersive mixing is developed and compared with experimental data. Next, simulation of both dispersive (rupture and erosion mechanisms) and distributive mixing is carried out and the performances of three batch mixers are compared.

EXPERIMENTS

As the in situ observation of carbon black dispersion in a mixer is impossible, a device has been built to perform such studies. As shown in fig. 1, two glass plates are counter-rotating and driven by independent motors. The polymer matrix between them contains few pellets. The distance between the two plates can be adapted to control the shear rate in the sample. A heating system allows the temperature control. A camera records each experiment for further investigation. For example, with erosion, an image analysis system is used to determine the pellet size at prescribed instants. In this paper, we mainly focus on the dispersion of N234 carbon black pellets in an SBR matrix at 140°C. As for rubber compounds, since the mixing time is short compared to infiltration time, the effect of infiltration is neglected.

Figure 2(a) shows a chronology of a typical erosion process. Similarly, figure 2(b) is a visualization of a rupture process. Both erosion and rupture examples shown in figure 2 are for the same level of shear stress but for two different initial sizes of the pellets. Based on a large set of experiments, where we modified initial sizes of pellets and shear stresses, we found out that the critical shear stress needed to get rupture of a pellet is inversely proportional to its initial size, figure 3:

$$\tau_c^{\text{rupture}} \propto \frac{1}{R_0} \quad (1)$$

For erosion mechanisms, different laws describing the evolution of the pellets size are available in the literature. Those laws have been determined with artificially built pellets suspended in a low viscosity Newtonian matrix. For example, we can cite the law of Kao and Mason [4]:

$$R_0^3 - R_t^3 = c_1 \dot{\gamma} t \quad (2)$$

and the law of Rwei at al. [5]:

$$\ln(R_t/R_0) = -c_2 \dot{\gamma} t \quad (3)$$

where R_0, R_t, c_1, c_2 , (latin γ with dot) and t are respectively the initial size of the pellet, the size at time t , two constants including the viscosity, the shear rate and the time.

Contrary to studies found in literature, we must note that, in our experiments, the pellets are commercial ones, introduced in the device untreated; moreover the matrix is highly viscoelastic, fig. 4. Erosion kinetics of N234 carbon black pellets in the SBR matrix seems to follow the model proposed by Kao and Mason. It allows gathering all the measurements on a single curve, as shown on fig. 5. Furthermore, it has been possible to express the coefficient c_1 as:

$$\text{If } \tau > \tau_c^{\text{erosion}} : c_1 = \alpha (\tau - \tau_c^{\text{erosion}}) \text{ else } c_1 = 0 \quad (4)$$

where τ is the shear stress and α and τ_c^{erosion} are two parameters characteristic of the filler/matrix system.

MATHEMATICAL MODEL [6]

Considering a small volume located in a position X in a mixer as shown in fig. 6, we define a mass density function (r, X, t) that is function of the agglomerate sizes r , the location X and the time t . As the material point X moves across the mixer, it is subjected to shear forces. Thus, the agglomerates attached to this point erode and break. The mass density function changes accordingly to reflect the variation in size distributions. Based on the erosion laws (2) and (3), we derived partial differential equations available for agglomerates distributions. The Kao and Mason law becomes:

$$\frac{\partial \rho}{\partial t} = \frac{\partial \rho}{\partial r} \frac{c_1}{3r^2} - \frac{c_1}{r^3} \rho \quad (5)$$

while the Rwei at al. law is:

$$\frac{\partial \rho}{\partial t} = \frac{\partial \rho}{\partial r} c_2 r - 3c_2 \rho \quad (6)$$

A special treatment is made for rupture since it should be considered as a discontinuous phenomenon. Let us assume that at time t , for a material point X , the local shear stress is T . Based on fig. 3, we get immediately the sizes of agglomerates that are breaking apart at this stress T . We assume that all of the agglomerates are broken into two equal fragments. Accordingly, the mass density function is modified.

To validate our approach we ran some experiments with rubber masterbatches containing around 20% in volume of carbon black. After having sheared the samples in a Mooney chamber for various times, we used the Dispergrader 1000NT^(TM) dispersion, as shown in fig. 7. In these experiments, the shear stress is too low to induce rupture. From the experimental results, we get mass density functions to compare with our models. In fig. 8, the results for a shear rate of $1s^{-1}$ are shown. The peak corresponding to the generation of very small fragments is not predicted. The models describe well the general trend of the slow decrease of the maximum of the mass density function. However, the shift of this maximum to lower sizes is better simulated with the equation (6). Unfortunately, this good agreement degrades if we compare results at higher shear rates. Despite their limitations, the models do provide useful information for the process engineer.

ROTORS EVALUATION

As an illustration, we will discuss the analysis and comparison of mixing performed by three different mixers, fig. 9 and table 1: the GK4N with Old Standard rotors, the GK4N with ZZ2 rotors and GK2N with PES3 rotors. The first two mixers have tangential rotors, while the last one has intermeshing rotors. Moreover, in order to compare them, we scaled the "PES3" case to get the same volume of fluid in the chambers. We assume that the chambers are fully filled and that there is no slip on the walls. Also, since the mixing time is rather short (20 seconds), thermal effects are neglected and the simulation is done isothermally. All rotors rotate at 30 rpm. The SBR viscosity is modeled by a Bird-Carreau law:

$$\eta(\dot{\gamma}) = \eta_{\infty} + (\eta_0 - \eta_{\infty}) \left(1 + \Lambda^2 \dot{\gamma}^2 \right)^{(n-1)/2} \quad (7)$$

where (γ with dot) is the shear rate, $\eta_0 = 10^6$ Pa.s, $\eta_{\infty} = 10$ Pa.s, $\Lambda = 10$ s and $n = 0.23$. We assume the flow is periodic in time so that we

can reduce the flow calculation to one rotation of the rotors (2 seconds simulated in 45 constant time steps). For the pathlines and mixing evaluation, we reuse the timely periodic flow field in loop to get information for the complete mixing time (20 seconds). The finite elements code POLYFLOW® is used to evaluate each flow field. The mesh superposition technique is used to handle the evolution of the flow domain as the rotors move [7]. To evaluate mixing, we distribute 1500 material points in the whole flow domain and compute their trajectories for 20 seconds. Along their pathlines, shear rates, shear stresses, and area stretch ratio are instantaneously evaluated [8].

A wealth of information may be extracted from the results. For example in table 2, by combining fig. 3 with shear stress along a given trajectory, we evaluate the fraction of N234 agglomerates of a given size broken in each mixer during the ten rotations of the rotors. Almost all particles above 30 μm are broken for the three mixers. Yet, some big agglomerates still exist after ten rotations. When looking at smaller particles, we observe the better performance of intermeshing rotors. Only 1/3 of the 15 μm particles are broken in tangential mixers while we reach 60% of broken particles with PES3 case. Using (5), we evaluate the evolution of the mass density function of agglomerate sizes attached to each material point. Next we average all those functions at each time to get the mean mass density function representative of the dispersive mixing in the whole mixer. Fig. 10 shows the evolution of this mean function for the PES3 case, based on trajectories of 500 material points. The initial distribution size is between 25 and 50 μm . Rupture has a big effect. The initial peak almost disappears and is shifted to medium size agglomerates. Then erosion takes place where the peak maximum (at 15 μm) decreases slowly while amounts of aggregates (fragments with size less than 2 μm) increase dramatically. By applying the same procedure to the three cases, we compare their final mean mass density functions (fig. 11): in all cases, we observe a small residual fraction of large agglomerates (smallest obtained with the OS case). The ZZ2 and OS cases have the same mean final curves, while the PES3 case presents the best dispersive mixing with the smallest fraction of agglomerates of size above 2 μm .

Distributive mixing is also evaluated. In a first approach, we count the fraction of material points that left its initial chamber, table 3. The ZZ2 case has the slowest transfer rate between chambers, while the PES3 is the best, followed closely by the OS. Another parameter is the stretching capability of the mixer, based on the evaluation of the area stretch ratio along trajectories. In table 4, we present the average of the natural logarithm of the area stretch ratio as a function of time for the three mixers: PES3 has the lead, followed by ZZ2 and OS has the lowest stretching performance. Thus, clearly the intermeshing PES3 case appears to provide the best dispersive and distributive mixing [9].

CONCLUSIONS

An experimental device has been built to study the life of single agglomerates placed in a shear flow. For both the erosion and rupture mechanisms and under various setups, the relationship existing between time, local stress and size of the agglomerates has been determined. A mathematical model has been built to predict the evolution of large sets of agglomerates. Based on a known flow field, the model can predict the evolution of a mass density distribution function of agglomerates. The Kao and Mason model is relevant for low concentration of carbon blacks, while the Rwei et al. model seems to better describe dispersion at higher concentrations. Further experiments are necessary to better understand and model the dispersion process when interactions between agglomerates are important.

Various numerical techniques have been combined to simulate mixing in batch mixers. Mesh superposition technique to determine the flow field, particle tracking, dispersion model and statistical analysis to simulate and quantify dispersive and distributive mixing. These techniques not only help in understanding the complex phenomena occurring during the dispersive and distributive mixing, but also enable testing of new ideas and eventually improve the mixing process. Clearly, the intermeshing rotors show better performances to disperse and distribute carbon black agglomerates. The simulations also show that a small fraction of large agglomerates remain undispersed, as is the case in reality.

ACKNOWLEDGEMENT

This work is supported by the European Community as part of the "Competitive and Sustainable Growth" program. The authors wish to thank all the partners including Harburg-Freudenberger Maschinenbau GmbH (previously ThyssenKrupp Elastomertechnik), Snecma Propulsion Solide, Optigrade-Techpro and T.U. Lodz for their collaboration in this project.

REFERENCES

1. B.R. Richmond, paper n° 158, meeting of the Rubber Division, American Chemical Society, Orlando, Florida (1993).
2. V. Collin, Etude rhéo-optique des mécanismes de dispersion du noir de carbone dans des élastomères, Thèse de Doctorat, Ecole des Mines de Paris, Sophia Antipolis, France, (2004).
3. V. Collin, E. Peuvrel-Disdier, *Elastomery*, 9, p. 9 (2005).
4. S. V. Kao, S. G. Mason, *Nature*, 253, p. 619 (1975).
5. S. P. Rwei, D. L. Feke, I. Manas-Zloczower, *Polym. Eng. Sci.*, 31, p. 558 (1991).
6. B. Alsteens, *Mathematical Modelling and Simulation of Dispersive Mixing*, PhD Thesis, Université Catholique de Louvain, Belgium (2005).
7. POLYFLOW v3.10.0 User's Guide, chapter 20, Fluent Benelux, Wavre, Belgium (2003).
8. J.M. Ottino, *The kinematics of mixing: stretching, chaos and transport*, Cambridge University Press, (1989).
9. T. Avalosse, B. Alsteens, V. Legat, *Elastomery*, 9, (2005).

KEYWORDS

Dispersive mixing, rubber, carbon black, model, batch mixers

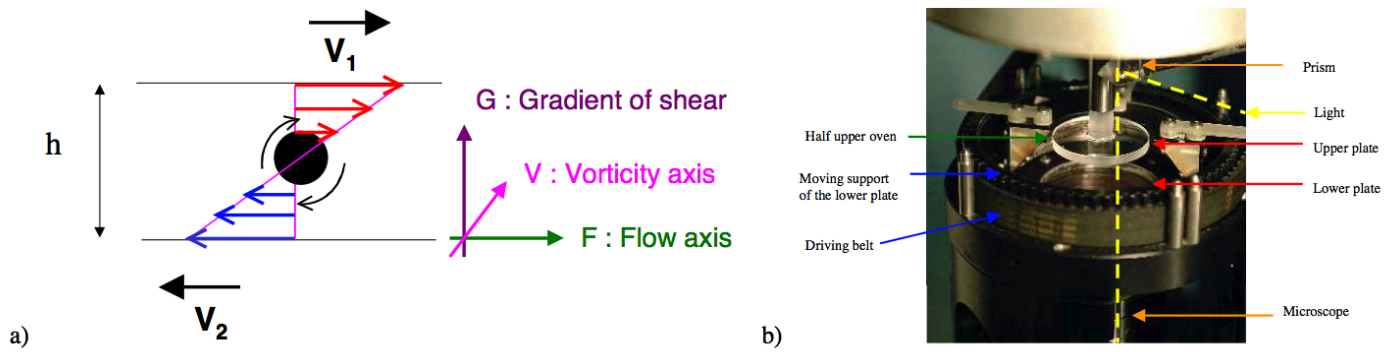


Figure 1: Counter-rotating device. a) Principle: in the counter-rotating geometry, the particle velocity can be fixed to zero relatively to the laboratory framework while the matrix is subjected to shear, b) View of the device

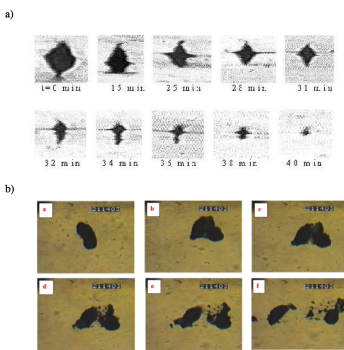


Figure 2: Dispersive mixing of N234 carbon black pellet in SBR under shear (shear rate = 6 s^{-1} , shear stress = 83900 Pa). a. Erosion ($R_0=22\mu\text{m}$). b. Rupture ($R_0=55\mu\text{m}$, rupture time = 6.76 seconds).

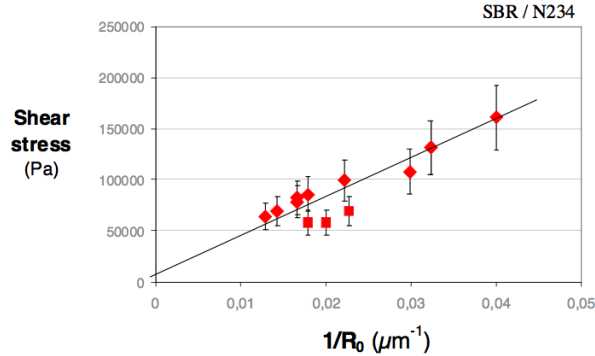


Figure 3: Critical shear stress for rupture versus the inverse of carbon black pellet radius. System N234 in SBR at 140°C

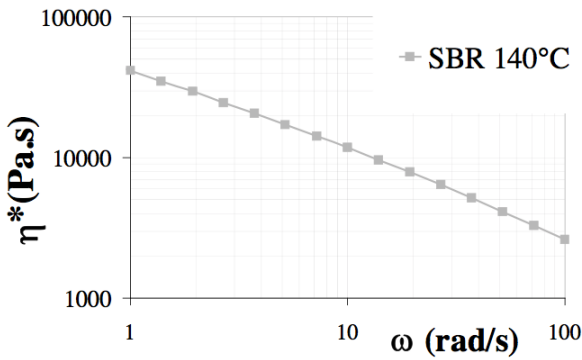


Figure 4: Complex viscosity (η^*) of SBR at 140°C

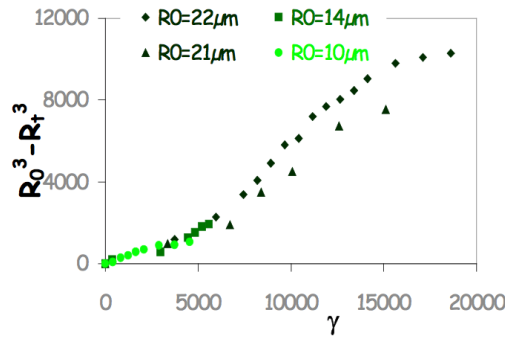


Figure 5: Erosion: evolution of the eroded volume as a function of the strain (shear rate = 7 s^{-1}) for various initial sizes of agglomerates. System N234 in SBR at 140°C

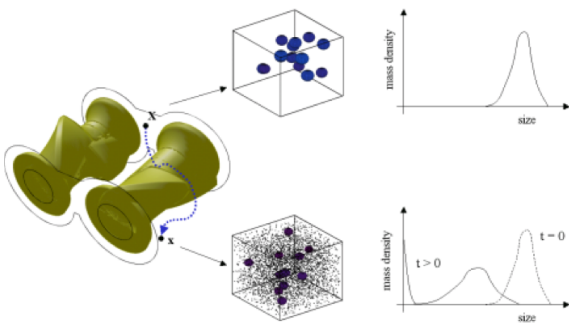


Figure 6: Evolution of the mass density distribution function for a material point moving in a batch mixer

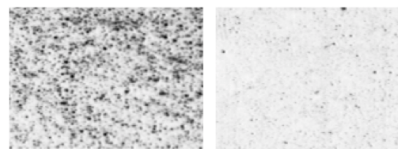


Figure 7: State of dispersion of carbon black agglomerates in rubber obtained with the Dispergrader 1000NTTM: (a) at the start of the experiment, (b) after 12 minutes of mixing.

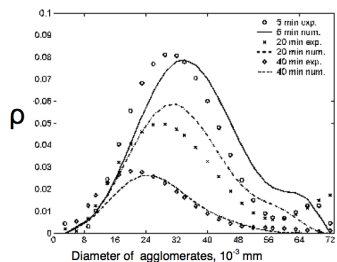
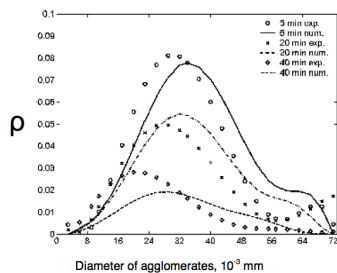


Figure 8: Evolution of the mass density distribution for experiments performed at 2rpm (shear rate = 1 s^{-1}), a) Kao & Mason, b) Rwei et al

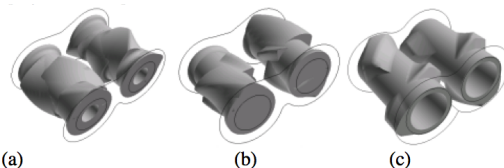


Figure 9: Rotors simulated: a) Old Standard rotors in a GK4N batch mixer, b) ZZ2 rotors in a GK4N batch mixer, c) PES3 rotors in a scaled batch mixer (in order to have same free volume as with the ZZ2 case).

Table 1. Dimensions of the mixers.

	OS	ZZ2	PES3
Diameter of each chamber (mm):	160	160	167
Depth of the chambers (mm):	208	208	224.1
Distance between axes (mm):	160	160	142.8
Volume of fluid (dm^3):	3.943	3.519	3.537
Torque (Nm), at 30 rpm:	2606	2650	3037

Table 2. Fraction of agglomerates of a given initial size broken at least once, after 20 seconds of mixing.

Agglomerate size:	15 μm	20 μm	30 μm
Rupture shear stress:	500 kPa	350 kPa	240 kPa
OS	32%	90%	> 98%
ZZ2	34%	90%	> 98%
PES3	56%	> 98%	> 99%

Table 3. Percentage of matter that moved – at least one time – from one chamber to the other one.

	t = 0 s.	t = 5 s.	t = 10 s.	t = 15 s.	t = 20 s.
OS	0%	42%	61%	71%	76%
ZZ2	0%	26%	44%	55%	62%
PES3	0%	47%	68%	77%	82%

Table 4. *Comparison of stretching capabilities.*

average $\ln(\lambda)$	OS	ZZ2	PES3
after 10 seconds	5.11	5.47	5.70
after 20 seconds	8.99	9.68	10.11

Return to [Best Papers](#).